TRIUMF	**UNIVERSITY OF ALBERTA EDMONTON, ALBERTA**	
	Date 2004/09/20	*File No.* TRI-DNA-04-5
Author GM Stinson		*Page* 1 *of* 14
Subject A further revision of the beam transport to the ISAC-II experimental area		

1. Introduction

Various studies of possible beam-transport configurations to the experimental hall of ISAC-II have been reported earlier [1–5]. In most of these investigations the intrinsic emittance of the beams extracted from the medium-β accelerator complex has been taken to be $\epsilon_0 = 0.2\pi$ mm-mr. It is anticipated that this intrinsic emittance would be increased to $\epsilon_0 = 0.3\pi$ mm-mr when the charge-state booster (CSB) is installed. Further, an estimate of the emittance variation as a function of the acceleration of the ions is now available. Consequently, it becomes necessary to investigate the effect of the emittance variation on beam profiles along the various beamlines. This report presents such a study.

The beamline configuration presented here is a slight modification of those presented earlier. In particular, the configuration has been modified to allow a future expansion that would permit one experiment to move back and forth between two target locations.

2. Emittance as a function of accelerated energy

Figure 1(a) shows the estimated variation of the emittance as a function of the accelerated energy of an ion over a range of energies from $0.5\,\mathrm{MeV}/\mu$ to $15\,\mathrm{MeV}/\mu$. Figure 1(b) is a similar plot over a range of energies from $0.5\,\mathrm{MeV}/\mu$ to $7\,\mathrm{MeV}/\mu$. The curves in cyan and marked $\epsilon_0 = 0.2\pi$ mm-mr correspond to the intrinsic emittances of the present ISAC ion sources. These may be taken as 2σ emittances for operation *without* the CSB [6]. Those in magenta and marked $\epsilon_0 = 0.3\pi$ mm-mr are estimated to be the intrinsic emittances for operation *with* the CSB. For this case the emittances also may be considered as emittances at the 2σ level [6].

Values for these curves were obtained by first computing the value of $\beta_i = v_i/c$ of an ion at an accelerated energy of $T_i\,\mathrm{MeV}/\mu$ using the relationship

$$\beta_i \;=\; \sqrt{\frac{T_i}{T_0}} \cdot \beta_0 \;,$$

where β_0 is the (known) value of β for the ion at an accelerated energy of $T_0\,\mathrm{MeV}/\mu$. Then if the intrinsic emittance of the beam at the energy T_0 is ϵ_0, the emittance ϵ_i at the energy T_i is obtained from

$$\epsilon_i \;=\; \frac{\epsilon_0}{\beta_i} \;.$$

In this case we use [6] $T_0 = 1.5\,\mathrm{MeV}/\mu$, $\beta_0 = 0.056$, and $\epsilon_0 = 0.2\pi($ or $0.3\pi)$ mm-mr.

3. General observations

3.1 An overview of the proposed configuration

The proposed layout of the experimental area of ISAC-II is shown in figure 2. The large rectangle indicates the extent of the experimental area; the short (cyan) vertical line represents the interior west wall of the accelerator vault.

The beamlines to the target locations labeled TGT1, TGT2, and TGT3 are considered as part of the initial installation, although that to TGT4 may be installed last. These beamlines are colored cyan. [Numbering of the targets is historical in that the target location TGT3 was initially assigned to a beamline that passed undeflected by the first dipole in the experimental hall—the ‘straight-through’ beamline. When it was first proposed none of the experimenters were interested in using such a beamline.]

During initial operation the TIGRESS experimental apparatus will be mounted at TGT1 and, eventually, the EMMA system will be located here. The TUDA experimental equipment will be installed at TGT2. Equipment for the HERACLES experiment will be located at the TGT3 position.

Beamlines to target locations labeled TGT5 and TGT6 are indicated as a possible future expansion in the experimental area. At that time the TUDA experiment will abandon TGT2 and move to the TGT6 location. The TIGRESS experiment will move to TGT5 and a rail system will be installed to allow it to move between the TGT5 and TGT1 locations.

We note at this point that although not shown in figure 2, a straight-through beamline and one similar to that leading to the HERACLES experiment could be installed emanating from the first dipole of the TGT5–TGT6 configuration.

3.2 An overview of the optics of the beamlines

The overall design of the system is to produce a doubly-achromatic double waist at all target locations *except* at the TGT4 position. At those positions one may have a beam spot with a 'nominal' diameter of either 1 mm or 2 mm. We put nominal in single quotes here because the design parameters in TRANSPORT fits were 0.9 mm for the 1 mm beam spot and 0.16 mm for the 2 mm beam spot.

In general, production of a 2 mm diameter beam spot is possible for most of the emittances that one would expect from the accelerator system. On the other hand, production of a beam spot 1 mm in diameter is possible only over a limited range of emittances. This is due to the apertures and strengths of the quadrupoles that are available *and* of the limited vertical (in particular) and horizontal apertures of the the dipole magnets and their existing vacuum boxes.

A doubly achromatic beam spot at the TGT4 location is not possible because of the single bend in this beamline. Consequently, the beam is first brought to a double focus 3 m downstream of the dipole. A quadrupole triplet is then used to produce a spatially undispersed ($R_{16} = 0$ but $R_{26} \neq 0$ in TRANSPORT notation), nominally 2 mm diameter beam spot at the target location.

This system of beamlines naturally breaks into two sections: that within the accelerator vault and those leading to the experimental targets. In terms of the labels in figure 2, the section of beamline within the accelerator vault is that between the location labeled β_{exit}, the exit of the medium-β accelerator complex, and the location labeled WST2. We consider the two quadrupoles downstream of WST2 as part of the beamlines to the experimental targets although they too are physically within the accelerator vault.

Within the accelerator vault and with reference to figure 2, the first four quadrupoles downstream of the medium-β exit bring the beam to a double waist at the position labeled WST0. A six-quadrupole $+\boldsymbol{I}$ section follows and translates the double waist at WST0 to an identical double waist at the WST1 location. The four-quadrupole section between WST1 and WST2 is a matching section

3.3 Specific design parameters and notation

The following parameters, notation, and limitations have been used in the designs reported here.

1. All calculations reported here have been made at a proton momentum of 0.93 GeV/c. This momentum corresponds[7)] to a proton energy of 0.3828 GeV or, equivalently, to an ion of mass 150 and $A/q = 7$ that is accelerated to an energy of 6.5 MeV/μ. The magnetic rigidity of such beams is 3.587 T-m.
2. Transport of multi-charged beams has *not* been considered.
3. All quadrupoles have been assumed to have an aperture radius of $a = 100$ cm and their pole-tip fields B_0 are given in kG. Consequently, the field gradient of a quadrupole g is given by $g = B_0/10$ T-m.

1. Quadrupoles in the accelerator vault are prefixed with the letter 'V' and are numbered sequentially from 1 to 14 beginning at the exit of medium-β accelerator complex.
2. The two quadrupoles downstream of WST2 are labeled Q1 and Q2 and are the first two quadrupoles of any beamline. Subsequent quadrupoles of a beamline are numbered sequentially beginning at Q3.
3. Looking in the beam direction the first dipole in the experimental area deflects beam 18.5° to the right to the TGT4 location or 30° to the left toward the TGT1 and TGT2 locations. This dipole is designated B1.

   The dipole on the 30° leg from B1 deflects beam 30° to the left toward TGT1 or 30° to the right toward TGT2. This dipole is designated B2.

   Similar dipoles in the future expansion shown in figure 2 are designated B3 and B4 respectively.

All quadrupoles are of the L2 type because a large number of these are available. In the listings of TRANSPORT input, pole-tip fields of the quadrupoles are given in kG and their half-apertures taken as 100 cm. Consequently, the gradients of the quadrupoles in T/m are simply found by dividing their pole-tip fields by 10.

For consistency with [1)] we continue to use the (non-standard) convention that a positive bend is one to the right when looking in the beam direction.

3. Details of the design

In the following sections we present the design of each line in more detail. A listing of TRANSPORT input for each section is given, as are the beam parameters and elements of the overall transfer matrix. A plot of the half-widths of the beam envelope is also given for each line.

3.1 The +60° beamline

In this section of beamline each dipole bends 30° to the left (looking along the beam direction) for a net deflection of the beam of +60°. As mentioned above, this beamline differs from that shown in figure 8 of ref[1)] by the addition of one quadrupole upstream of the first +30° dipole and another symmetrically placed downstream of the second +30° dipole. An input listing for the TRANSPORT program is given in table 1. Beam sizes and elements of the overall transfer matrix are given at the midpoint and target locations in table 5a. Figure 3 is a plot of the calculated half-widths of the beam in the horizontal (x) and vertical (y) planes. Note that the vertical half-width is plotted as a negative quantity.

From table 5a it is seen that at the midpoint of this beamline there is simultaneous point-to-point and waist-to-waist imaging in the horizontal plane. There the dispersion is $-2.3934\,\mathrm{cm}/\%$. In the vertical plane there is simultaneous parallel-to-point and waist-to-waist imaging. At the target location the overall transfer matrix is $+\boldsymbol{I}$ in the horizontal plane and $-\boldsymbol{I}$ in the vertical plane. Thus this beamline could be used for the transport of a multi-charged beam.

3.2 The +0° beamline

In this configuration the first dipole bends +30° to the left and the second bends −30° to the right for a net deflection of the beam of 0°. TRANSPORT input for this case is given in table 2. The calculated beam sizes at the midpoint and target location of this configuration are also given in table 5a. Figure 4 shows the half-widths of the beam profile throughout the beamline.

At the midplane there is a double waist. From table 5a it is seen that there is almost a double focus as well (R_{12} and R_{34} approximately zero). Here the beam is horizontally achromatic in space ($R_{16} = 0$) but dispersed in angle ($R_{26} \neq 0$). At the target location the beam spot is a doubly-achromatic double waist. There also is (almost) a double focus here.

3.3 The straight-through beamline

As its name implies both dipoles are turned off so that the beam passes undeflected through the first dipole. In order for a multi-charged beam to be directed to a target on this line it is necessary that the overall the first and second dipole.

A TRANSPORT listing for this unit section is given in table 3. Note that in this listing a second shorter unit section is appended to the six-quadrupole one. Table 5b lists the beam parameters at the first and second foci. Figure 5 shows the half-widths of the beam throughout the beamline.

3.4 The −18.5° beamline

This beamline uses the −18.5° port of the first dipole. The design is such that a double focus is produced at location F1 and a circular beam spot nominally 3 mm in diameter is produced at the TGT4 location. There the beam is spatially achromatic ($R_{16} = 0$) but is dispersed in angle.

Table 4 lists the TRANSPORT input for this beamline. Beam parameters and elements of the overall transfer matrix are given in table 5b. Figure 6 shows the half-widths of the beam throughout the beamline.

The beam cannot be made doubly achromatic at the TGT4 location because the initial beam has been assumed achromatic and only one dipole is involved. However, the beam transport could be modified to produce other beam spots at the target location—or at another target location—if required.

4. Discussion

This report has presented an updated design for beam transport to the ISAC-II experimental area. Two of the beamline sections—the +60° line and the straight-through line—are suitable for the transport of a multi-charged beam.

Initial installation of th +60° and +0° beamlines would require only ten power supplies. The three for the last quadrupoles of these lines could be switched from one line to the other.

It should be noted, however, that all ten of the supplies should be either bipolar or equipped with reversing switches.

References

1. G. M. Stinson, *An additional beamline in the* ISAC-II *experimental area*, TRIUMF report TRI-DNA-04-3, March, 2004.

2. G. M. Stinson, *Beam transport from the medium β exit to beam transport to the* ISAC-II *experimental area*, TRIUMF report TRI-DNA-04-2, February, 2004.

3. G. M. Stinson, *A revision of beam transport to the* ISAC-II *experimental area*, TRIUMF report TRI-DNA-04-1, January, 2004.

4. Z. H. Peng and R. E. Laxdal, *A Design Layout for ISAC-II Post-SCLinac Beamline (HEBT-II)*, TRIUMF report TRI-DN-01-xx, December, 2003.

5. G. M. Stinson, *On the use of existing magnets during the initial operation of the* ISAC-II *experimental area*, TRIUMF report TRI-DNA-03-1, March, 2003.

6. R. E. Laxdal, *Private communication*, TRIUMF, December, 2003.

7. G. M. Stinson, *A preliminary study of beam transport to the* ISAC-II *experimental area*, TRIUMF report TRI-DNA-01-4, September, 2001.

Table 1

TRANSPORT input for the +60° (+30°+30°) system

'ISAC-II AECL +30+30 deg - 10Q Unit to Double Waists - 2.2 m - 2004/01/13 '					
0					
13.		12.00000;			
16.00	G/2	5.00000	2.50000;		
16.00	K1	7.00000	0.45000;		
16.00	K2	8.00000	2.80000;		
1.000000	BEAM	0.10000	2.00000	0.10000	2.00000
		0.00000	0.10000	0.93000;	
3.0		2.20000;			
5.00	Q1	0.32500	102.50866	100.00000;	
3.0		0.30000;			
5.00	Q2	0.32500	114.48215	100.00000;	
3.0		0.32000;			
3.0	WALL	0.78740;			
3.0		0.32000;			
5.00	Q3	0.32500	−47.09907	100.00000;	
3.0	B1IN	0.67500;			
20.0		180.00000;			
2.0		0.00000;			
4.000	B1	1.04720	15.51050	0.00000;	
2.0		0.00000;			
20.0		−180.00000;			
3.0	B1EX	0.00001;			
3.0		1.80000;			
5.00	Q4	0.32500	−96.87130	100.00000;	
3.0		0.30000;			
5.00	Q5	0.32500	76.51190	100.00000;	
3.0	MID	0.92500;			
3.0		0.92500;			
5.00	Q6	0.32500	76.51190	100.00000;	
3.0		0.32000;			
5.00	Q7	0.32500	−96.87130	100.00000;	
3.0	B2IN	1.80000;			
20.0		180.00000;			
2.0		0.00000;			
4.000	B2	1.04720	15.51050	0.00000;	
2.0		0.00000;			
20.0		−180.00000;			
3.0	B2EX	0.00001;			
3.0		0.67500;			
5.00	Q8	0.32500	−47.09907	100.00000;	
3.0		0.32000;			
3.0		0.78740;			
3.0		0.32000;			
5.00	Q9	0.32500	114.48215	100.00000;	
3.0		0.30000;			
5.00	Q10	0.32500	102.50866	100.00000;	
3.0	F2	2.20000;			
SENTINEL					
SENTINEL					

Table 2

TRANSPORT input for the +0° (+30°−30°) system

'ISAC-II AECL +30-30 deg - 10Q to Double Achromatic Waists - 2.2 m - 2004/01/13 '					
0					
13.		12.00000;			
16.00	G/2	5.00000	2.50000;		
16.00	K1	7.00000	0.45000;		
16.00	K2	8.00000	2.80000;		
1.000000	BEAM	0.10000	2.00000	0.10000	2.00000
		0.00000	0.10000	0.93000;	
3.0		2.20000;			
5.00	Q1	0.32500	102.50866	100.00000;	
3.0		0.30000;			
5.00	Q2	0.32500	−125.64016	100.00000;	
3.0		0.32000;			
3.0	WALL	0.78740;			
3.0		0.32000;			
5.00	Q3	0.32500	98.92205	100.00000;	
3.0	B1IN	0.67500;			
20.0		180.00000;			
2.0		0.00000;			
4.000	B1	1.04720	15.51050	0.00000;	
2.0		0.00000;			
20.0		−180.00000;			
3.0	B1EX	0.00001;			
3.0		1.80000;			
5.00	Q4	0.32500	129.25079	100.00000;	
3.0		0.30000;			
5.00	Q5	0.32500	−85.01575	100.00000;	
3.0	MID	0.92500;			
3.0		0.92500;			
5.00	Q6	0.32500	−85.01575	100.00000;	
3.0		0.32000;			
5.00	Q7	0.32500	129.25079	100.00000;	
3.0	B2IN	1.80000;			
−20.0		180.00000;			
2.0		0.00000;			
4.000	B2	1.04720	15.51050	0.00000;	
2.0		0.00000;			
−20.0		−180.00000;			
3.0	B2EX	0.00001;			
3.0		0.67500;			
5.00	Q8	0.32500	98.92205	100.00000;	
3.0		0.32000;			
3.0		0.78740;			
3.0		0.32000;			
5.00	Q9	0.32500	−125.64016	100.00000;	
3.0		0.30000;			
5.00	Q10	0.32500	102.50866	100.00000;	
3.0	F2	2.20000;			
SENTINEL					
SENTINEL					

Table 3

TRANSPORT input for the straight-through (+0°+0°) system

'ISAC-II AECL +30-30 deg - 10Q to Double Achromatic Waists - 2.2 m - 2004/01/13 '					
0					
13.		12.00000;			
16.00	G/2	5.00000	2.50000;		
16.00	K1	7.00000	0.45000;		
16.00	K2	8.00000	2.80000;		
1.000000	BEAM	0.10000	2.00000	0.10000	2.00000
		0.00000	0.10000	0.93000;	
3.0		2.20000;			
5.00	Q1	0.32500	107.36949	100.00000;	
3.0		0.30000;			
5.00	Q2	0.32500	−107.36949	100.00000;	
3.0	MID1	2.20000;			
3.0		2.20000;			
5.00	Q3	0.32500	107.36949	100.00000;	
3.0		0.30000;			
5.00	Q4	0.32500	−107.36949	100.00000;	
3.0	MID2	2.20000;			
3.0		2.20000;			
5.00	Q5	0.32500	107.36949	100.00000;	
3.0		0.30000;			
5.00	Q6	0.32500	−107.36949	100.00000;	
3.0	F1	2.20000;			
−10.0		−1.00000	1.00000	1.00000	0.00100;
−10.0		−1.00000	2.00000	0.00000	0.00100;
−10.0		−2.00000	1.00000	0.00000	0.00100;
−10.0		−2.00000	2.00000	1.00000	0.00100;
−10.0		−3.00000	3.00000	1.00000	0.00100;
−10.0		−3.00000	4.00000	0.00000	0.00100;
−10.0		−4.00000	3.00000	0.00000	0.00100;
3.0		1.00000;			
5.00	Q3	0.32500	126.88231	100.00000;	
3.0		0.30000;			
5.00	Q4	0.32500	−126.88231	100.00000;	
3.0	MID3	1.00000;			
3.0		1.00000;			
5.00	Q5	0.32500	126.88231	100.00000;	
3.0		0.30000;			
5.00	Q6	0.32500	−126.88231	100.00000;	
3.0	F2	1.00000;			
−10.0		−1.00000	1.00000	1.00000	0.00100;
−10.0		−1.00000	2.00000	0.00000	0.00100;
−10.0		−2.00000	1.00000	0.00000	0.00100;
−10.0		−2.00000	2.00000	1.00000	0.00100;
−10.0		−3.00000	3.00000	1.00000	0.00100;
−10.0		−3.00000	4.00000	0.00000	0.00100;
−10.0		−4.00000	3.00000	0.00000	0.00100;
SENTINEL					
SENTINEL					

Table 4

TRANSPORT input for the −18.5° system

'ISAC-II AECL – -18.5 deg – 3 mm diameter and $R_{16} = 0 at F2$ – 04/01/14'					
0					
13.		12.00000;			
16.00	G/2	5.00000	2.50000;		
16.00	K1	7.00000	0.45000;		
16.00	K2	8.00000	2.80000;		
1.000000	BEAM	0.10000	2.00000	0.10000	2.00000
		0.00000	0.10000	0.93000;	
3.0		2.2000;			
5.00	Q1	0.32500	159.94370	100.00000;	
3.0		0.30000;			
5.00	Q2	0.32500	−137.21811	100.00000;	
3.0		0.32000;			
3.0	WALL	0.78740;			
3.0		0.32000;			
5.00	Q3	0.32500	94.73307	100.00000;	
3.0		0.30000;			
3.0	B1IN	0.37500;			
−20.0		180.00000;			
2.0		0.00000;			
4.000	B1	1.06262	9.42604	0.00000;	
2.0		0.00000;			
−20.0		−180.00000;			
3.0	B1EX	0.00001;			
3.0		1.00000;			
3.0		1.80000;			
3.0	F1	1.80000;			
−10.0		−1.00000	2.00000	0.00000	0.00100;
−10.0		−3.00000	4.00000	0.00000	0.00100;
3.0		1.00000;			
3.0		1.00000;			
3.0		1.00000;			
5.00	Q4	0.32500	80.34370	100.00000;	
3.0		0.30000;			
5.00	Q5	0.32500	−141.36654	100.00000;	
3.0		0.30000;			
5.00	Q6	0.32500	88.60354	100.00000;	
3.0		1.00000;			
3.0		1.00000;			
3.0	F2	1.00000;			
−10.0		−1.00000	6.00000	0.00000	0.00100;
−10.0		1.00000	1.00000	0.10000	0.00100;
−10.0		3.00000	3.00000	0.10000	0.00100;
SENTINEL					
SENTINEL					

Table 5a

Predicted beam sizes and overall transfer matrices at the experimental locations on the +60° and 0° beamlines — Doublet in vault, one quadrupole added

Parameter	+60° leg		0° leg	
	at MID	at TGT1	at MID	at TGT2
$\pm x$ (cm)	0.314	0.100	0.048	0.100
$\pm\theta$ (mr)	0.984	2.000	4.230	2.000
$\pm y$ (cm)	0.201	0.100	1.147	0.101
$\pm\phi$ (mr)	0.994	2.000	0.174	1.986
R_{11} (cm/cm)	−2.0326	1.0000	0.4743	0.9810
R_{12} (cm/mr)	−0.0004	0.0004	−0.0023	−0.0097
R_{16} (cm/%)	−2.3934	0.0000	0.0000	0.0000
R_{21} (mr/cm)	−0.0001	0.0003	4.0936	3.8834
R_{22} (mr/mr)	−0.4920	1.0000	2.0882	0.9810
R_{26} (mr/%)	0.0001	−0.0003	5.3372	0.0000
R_{33} (cm/cm)	0.0000	−1.0000	−7.2269	−0.1985
R_{34} (cm/mr)	−0.1006	−0.0001	−0.4452	0.0494
R_{43} (mr/cm)	9.9413	0.0000	1.3461	−19.4567
R_{44} (mr/mr)	0.0006	−1.0000	−0.0555	−0.1985

Table 5b

Predicted beam sizes and overall transfer matrices at the experimental locations on straight-through and −18.5° beamline — Doublet in vault, one quadrupole added

Parameter	Straight-through leg		−18.5° leg	
	at F1	at F2	at F1	at TGT4
$\pm x$ (cm)	0.100	0.100	0.261	0.150
$\pm\theta$ (mr)	2.000	2.000	1.369	1.875
$\pm y$ (cm)	0.100	0.100	0.277	0.150
$\pm\phi$ (mr)	2.000	2.000	0.965	1.476
R_{11} (cm/cm)	1.0000	−1.0000	2.3586	0.5853
R_{12} (cm/mr)	0.0000	0.0000	0.0000	0.0690
R_{16} (cm/%)	0.0000	0.0000	1.1220	−0.0001
R_{21} (mr/cm)	0.0000	0.0000	10.2648	−16.6656
R_{22} (mr/mr)	1.0000	−1.0000	0.4240	−0.2576
R_{26} (mr/%)	0.0000	0.0000	3.1730	−6.8890
R_{33} (cm/cm)	1.0000	−1.0000	−2.7702	−0.5072
R_{34} (cm/mr)	0.0000	0.0000	0.0000	−0.0706
R_{43} (mr/cm)	0.0000	0.0000	−6.4032	14.6866
R_{44} (mr/mr)	1.0000	−1.0000	−0.3610	0.0727

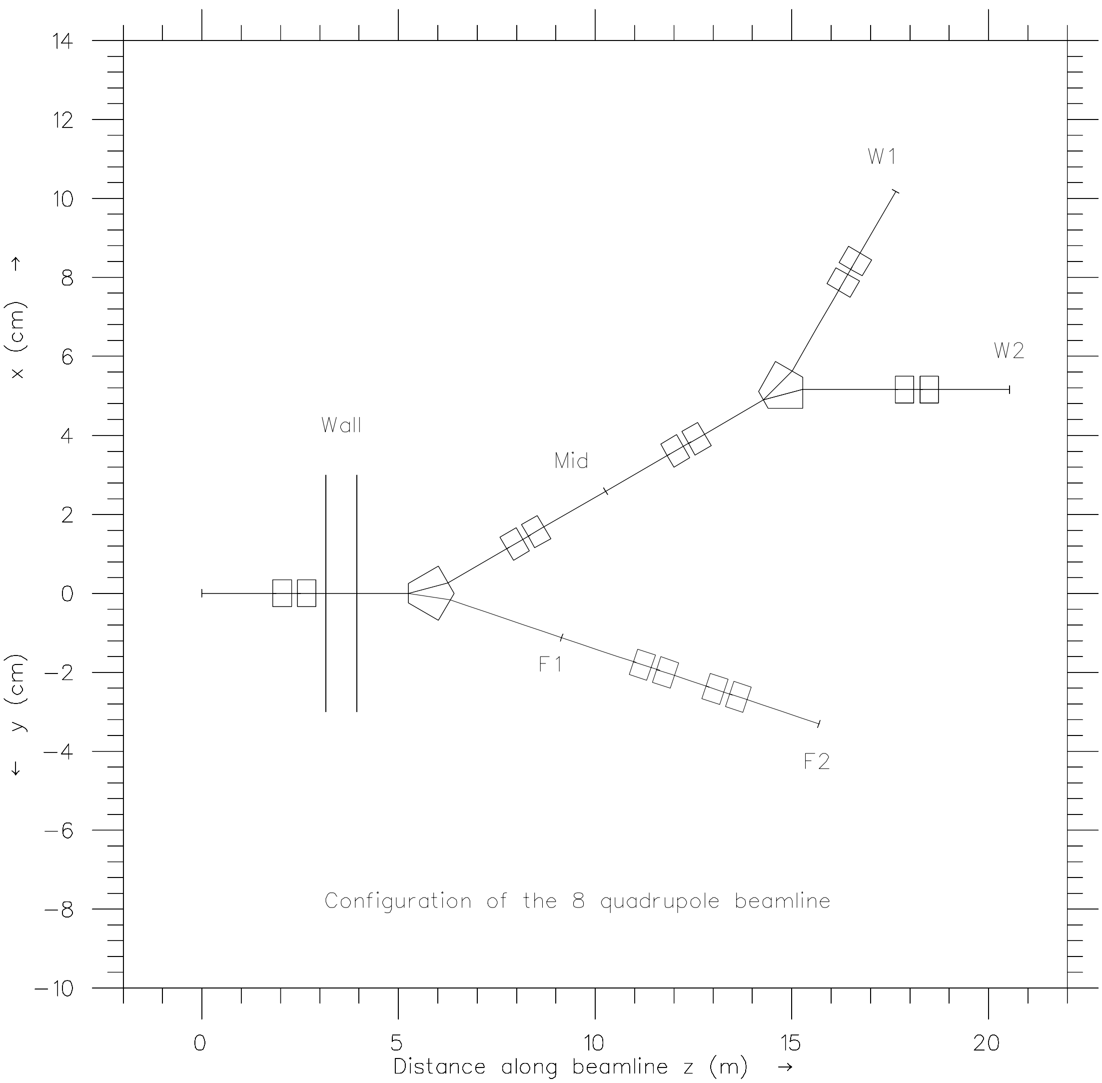

Fig. 1. The beamline configuration selected from reference 1.

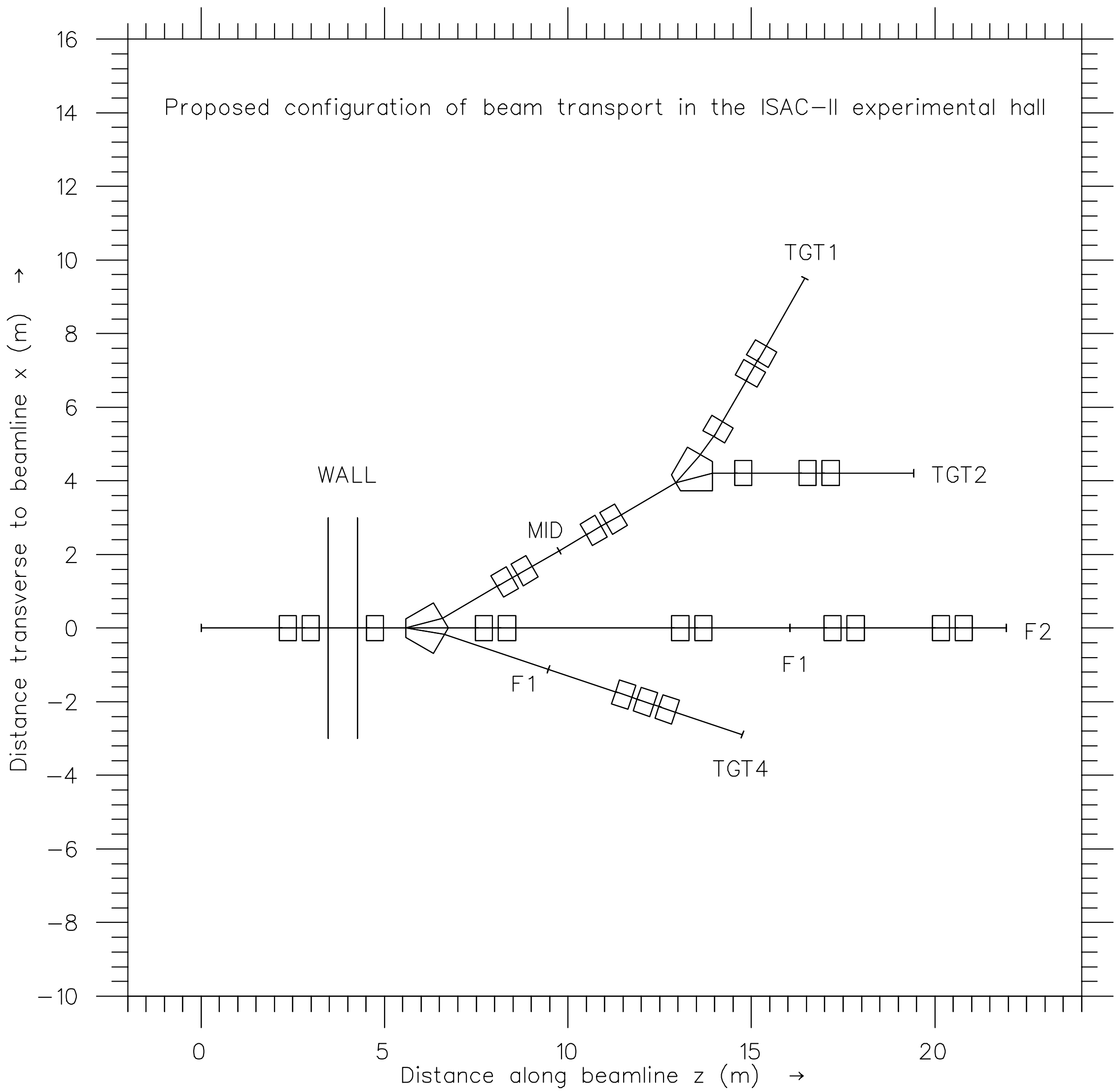

Fig. 2. The modification of the beam-transport configuration proposed in this report.

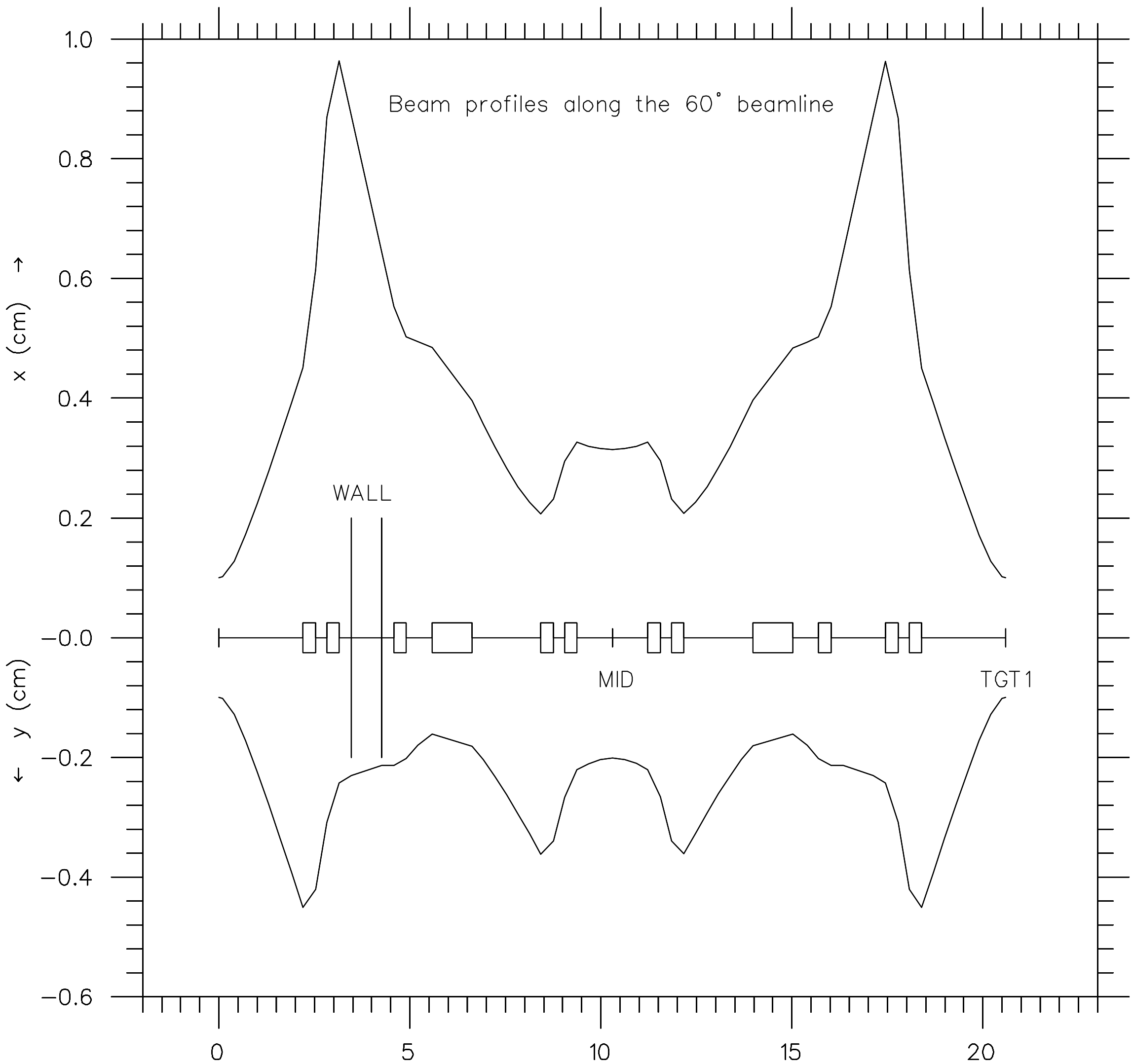

Fig. 3. Beam envelopes on the +60° beamline — Doublet in vault and added quadrupoles.

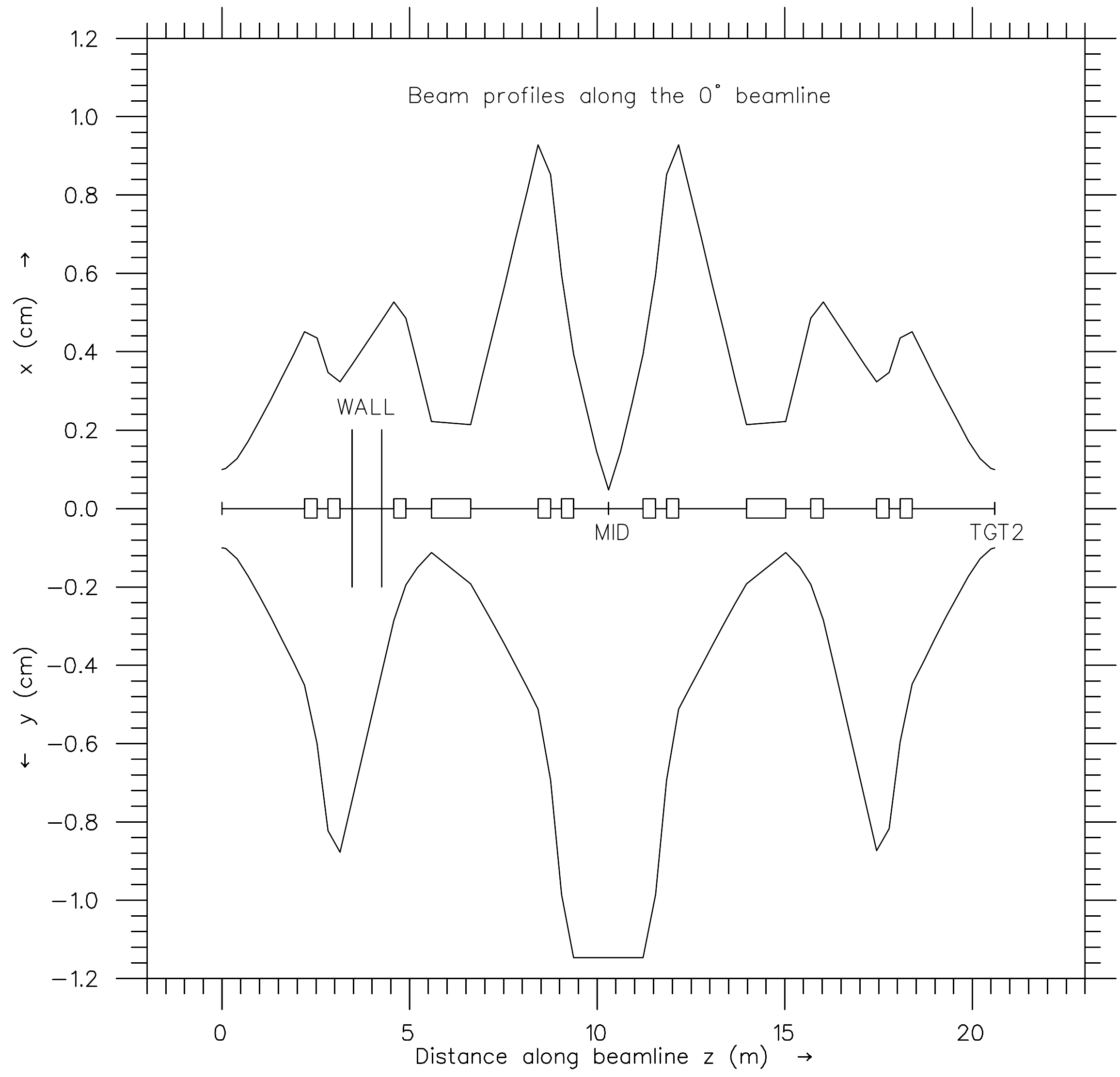

Fig. 4. Beam envelopes on the +0° beamline — Doublet in vault and added quadrupoles.

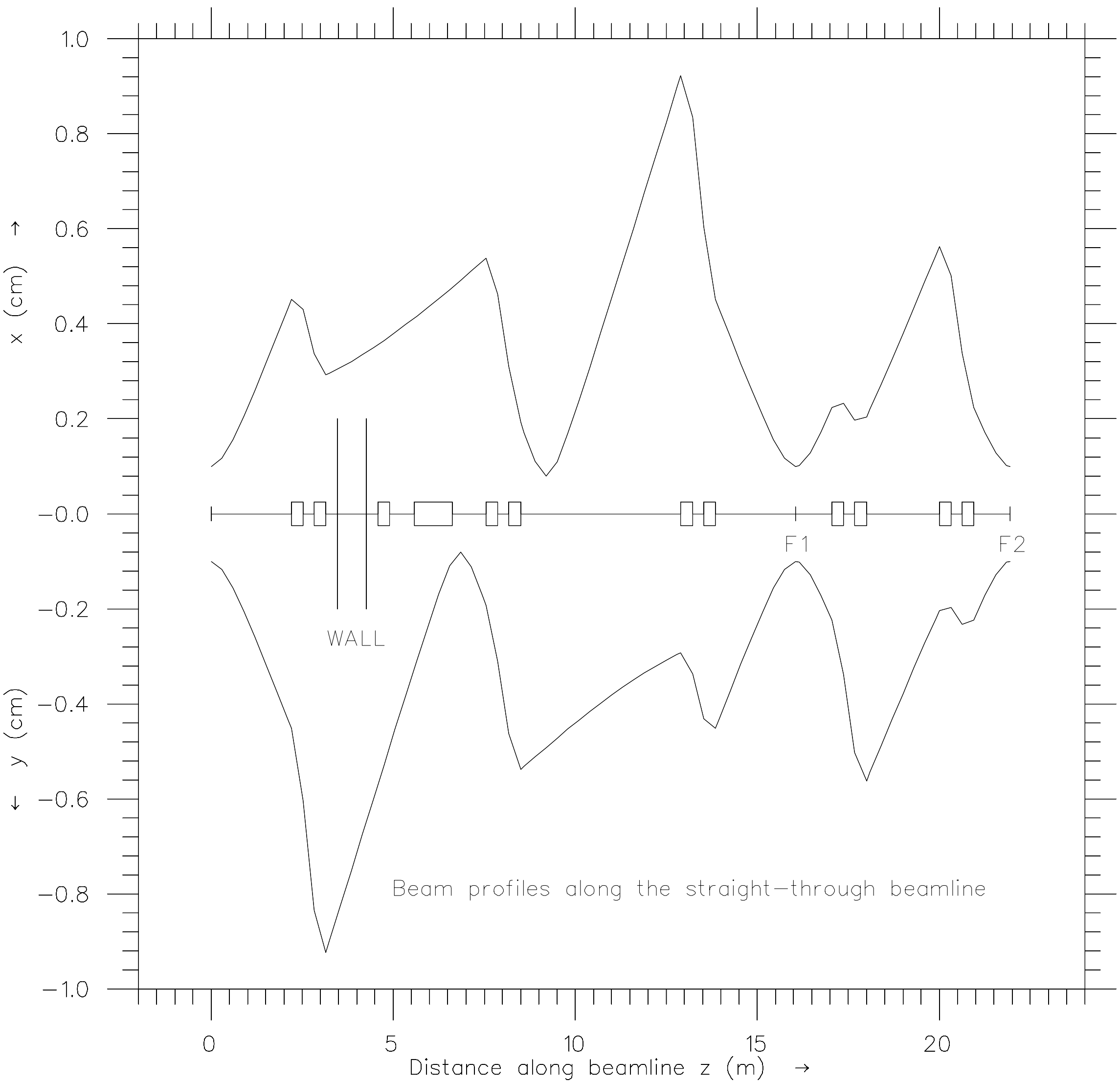

Fig. 5. Beam envelopes on the straight-through beamline — Doublet in vault and added quadrupoles.

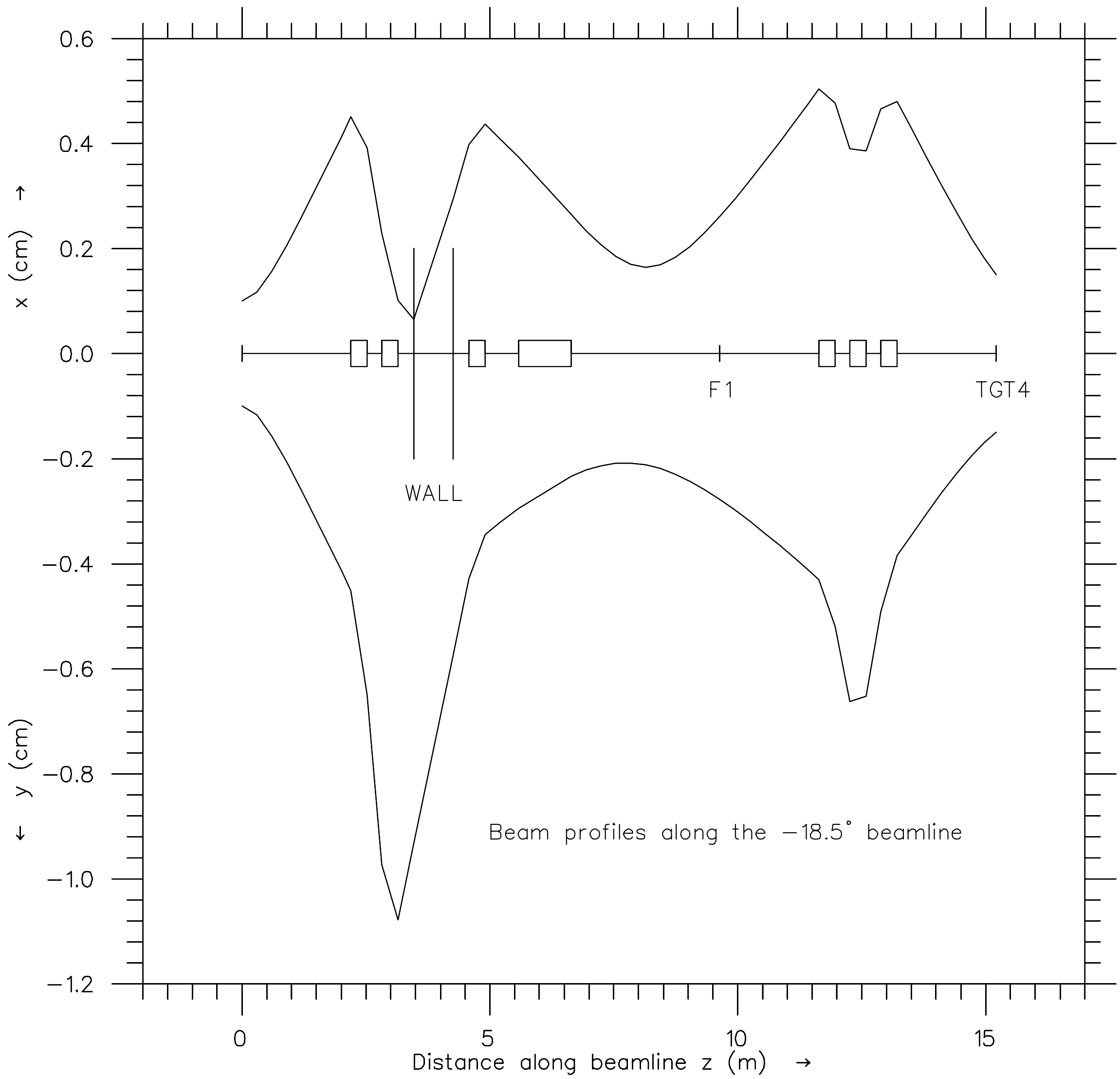

Fig. 6. Beam envelopes on the −18.5° beamline — Doublet in vault and added quadrupoles.